2005

Broadband Static Micro-Delay lines generation for OCT

Kamal Alameh
Edith Cowan University

David Sampson

Zhenglin Wang
Edith Cowan University

Rong Zheng
Edith Cowan University

Chung Poh
Edith Cowan University

Broadband Static Micro-delay lines generation for OCT

Kamal Alameh, David Sampson*, Zhenglin Wang, Rong Zheng and ChungKiak Poh
Centre for MicroPhotonic Systems, Electron Science Research Institute
Edith Cowan University, Joondalup, WA, Australia.
* Optical & Biomedical Engineering Laboratory, School of Electrical, Electronics and Computer Engineering, University of Western Australia, CRAWLEY, WA Australia.
Email: k.alameh@ecu.edu.au

Abstract

In this paper, we propose a novel technique to generate variable true time micro-delay for fibre-based optical coherent tomography (OCT) using two Opto-VLSI processors. The technique offers broadband high resolution scanning depth without moving parts. The beam steering and multicasting capabilities of the Opto-VLSI processors provide a valuable scanning tool allowing the delay generator to jump between nonadjacent depths and realising multiple delays simultaneously. Experimental results achieved maximum 500 μm delay with 3dB bandwidth is more than 55 nm at centre wavelength 1550nm.

1. Introduction

Optical coherence tomography (OCT) is a non-invasive technique that uses low-coherence reflectometry to detect the interference between a probe optical signal and a delayed reference signal, thus achieving optical imaging of detecting target. The low coherent broadband source makes the optical image very sensitive to path different between probe signal and delayed reference signal, so this technology can achieve high resolution along image depth [1]. There are many different ways to generate variable optical delay in OCT systems, most fibre-based OCT systems use mechanically-scanned optical components to delay the reference signal over a few millimetres with a few micron resolution [2-5]. However, to realise a robust OCT system, it is desirable to scan the reference path length with no moving parts. N. A. Riza demonstrated an acousto-optic (AO) scanning heterodyne interferometer [6] coupled with an acousto-optically switched high speed optical delay lines [7] for OCT system. The system can achieve sub-micro-second per data point sampling rate speed, but it is hard to obtain high scanning resolution, because a fixed step multi mirror assembly is used in the reference arm [8]. The use of 3-D electronic holography with fixed reference mirror [9], [10] has also been reported for OCT. It used a stationary Fourier-transform spectrometer in conjunction with an acousto-optical scanner to scan in both the transverse and depth dimensions. This technique requires a diode-array spectrometer, rather than a single photodiode, to record a correlogram, whose Fourier transformation yields the reflectivity profile of the tissue in the depth dimension.

In this paper, we present a novel broadband motion-free micro-delay generator for OCT, which uses two Opto-VLSI processors operating in the steering mode to generate variable true time delays suitable for high resolution OCT imaging. The multicasting capability of the Opto-VLSI processors provides a valuable diagnostic tool allowing multiple delays to be realised simultaneously [11].

2. Opto-VLSI processor

An Opto-VSLI processor is an array of liquid crystal (LC) cells whose crystallographic orientations are independently addressed by a Very-Large-Scale-Integrated (VLSI) circuit to create a reconfigurable, reflective, holographic diffraction grating plate. Application of voltage between the electrodes of the VLSI circuit induces a phase hologram in the LC layer, resulting in optical beam steering and/or beam shaping. Fabricated Opto-VLSI devices are electronically controlled, software-configured, polarisation independent, cost effective because of the high-volume manufacturing capability of VLSI as well as the capability of controlling multiple fibre ports in one compact Opto-VLSI module, and very reliable since beam steering is achieved with no mechanically moving part. These features open the way for numerous reconfigurable optical components. Fig. 1(a) shows a typical layout of an Opto-VLSI processor. Also shown is typical LC cell design. Usually Indium-Tin Oxide (ITO) is used as the transparent electrode, and evaporated aluminium is used as reflective electrode. The ITO layer is generally grounded and a voltage is applied at the reflective electrode by the VLSI circuit below the LC layer. Opto-VLSI processors can generate stepped blazed grating for optical beam steering, as well as multicasting grating for arbitrary beam splitting, where the diffraction orders are deliberately enhanced to generate an arbitrary beam splitting profile [11]. Recent

advances in nematic LC materials and Layer thickness control have allowed the incorporation of a thin quarter-wave-plate (QWP) layer between the LC and the aluminum mirror to accomplish polarization-insensitive multi-phase-level Opto-VLSI processors. These attractive capabilities of Opto-VLSI processors make them ideal platforms for reconfigurable optical components. Fig. 1(b) illustrates the steering and multicasting capability of Opto-VLSI processors.

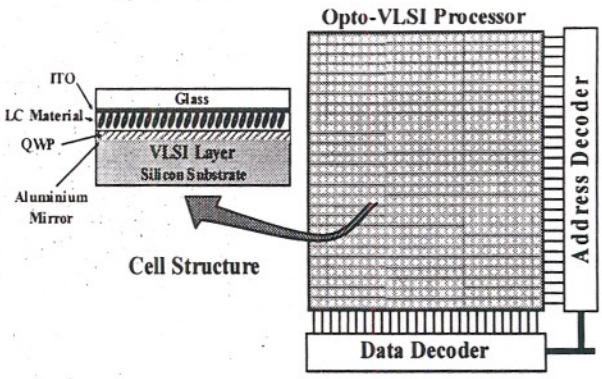

(a)

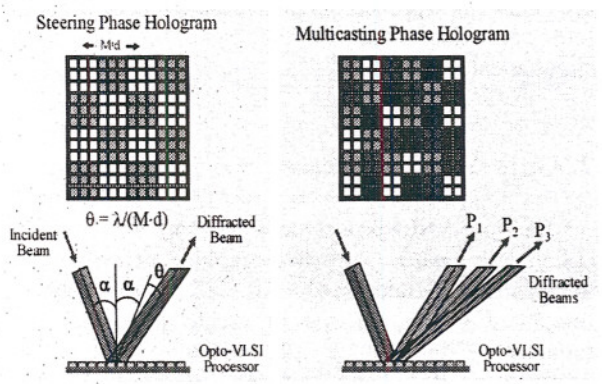

(b)

Fig. 1 (a) Typical Opto-VLSI processor and an LC cell structure design, (b) Steering and multicasting capabilities of an Opto-VLSI processor.

For a small incidence angle, the maximum steering angle of the Opto-VLSI processor is given by:

$$\theta_{\max} = \frac{\lambda}{M \cdot d} \qquad (1)$$

Where M is the number of phase levels, d is the pixel size, and λ is the wavelength. For example, an 8-phase Opto-VLSI processor having a pixel size of 1.8 microns can steer a 1550 nm laser beam by a maximum angle of around ±5.6° with a diffraction efficiency of 94%. The maximum diffraction efficiency of an Opto-VLSI processor depends on the number of discrete phase levels that the VLSI can accommodate. The theoretical maximum diffraction efficiency is given by [12]

$$\eta = \mathrm{sinc}^2\left(\frac{\pi n}{M}\right) \qquad (2)$$

Where $n = gM + 1$ is the diffraction order ($n = 1$ is the desired order), and g is an integer. The higher diffraction orders (which correspond to the cases $g \neq 0$) are usually unwanted crosstalks, which must be attenuated or properly routed outside the output ports to maintain a high signal-to-crosstalk performance.

3. Micro delay generation

Fig. 2 shows the broadband motionless micro-delay generator. It uses two Opto-VLSI processors without mechanical movable parts, in conjunction with an input fibre collimator that collimates the input beam, and an optical substrate that integrates the optical components in a robust assembly.

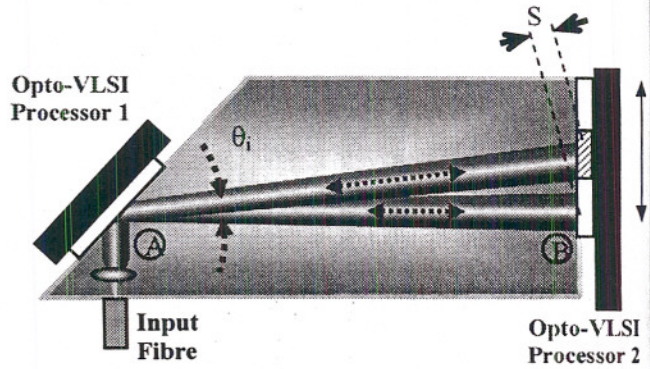

Fig. 2 Broadband motionless micro-delay generator

The first Opto-VLSI processor is placed face to face to the second opto-VLSI processor. Both Processors are driven by phase holograms that steer the optical beam by different angles. With no phase holograms on both Opto-VLSI processors, the input collimated optical beam is reflected horizontally from the surface of first Opto-VLSI along the path AB and reflected back from the surface of second Opto-VLSI along the same optical path BA, thus resulting in a minium round-trip optical path length. The minimum delay time corresponding to that minimum round-trip optical path length is taken as a reference delay. To generate a differential true-time delay, L_i, the collimated beam from the input fiber is steered an angle θ_i by the first Opto-VLSI processor while the second Opto-VLSI processor is driven with an appropriate phase hologram that steers the optical beam anticlockwise by an angle $2\theta_i$ thus reflecting the beam back along the incidence direction. The differential length delay, L_i, is given by:

$$L_i = 2\left[\frac{D \cdot n}{\sin(\theta_i)} - \frac{D \cdot n}{\tan(\theta_i)}\right] \quad (3)$$

Where D is the beam separation on the second Opto-VLSI processor, θ_i is beam steering angle from the first Opto-VLSI processor, and n is the substrate refractive index between the two Opto-VLSI processors. Equation (3) shows that the maximum achievable differential delay time is determined by the maximum steering angle of the Opto-VLSI processor, θ_{max}, and its active length D. If θ_{max} = 5.6° and D=10mm, then the maximum differential delay length is around 1 mm. Note that the proposed micro-delay generator allows any scanning depth to be dynamically generated without the need to go through intermediate depths. This is simply done by driving the Opto-VLSI processors with appropriate steering holograms. Note also, that the proposed structure can achieve multi-depth scanning using the multicasting capability of the Opto-VLSI processor [11].

4. Experimental setup

Fig. 3 shows the experimental setup for a proof-of-concept variable micro-delay generator. The two Opto-VLSI processors used in the experiment are commercially available one-dimensional liquid crystal devices produced by Boulder Nonlinear System, Inc (BNC), each consists of 4096 individually addressable nematic-phase liquid crystal pixels (pixel pitch is 1.8μm and length 7.3 mm), and has a maximum steering angle of around 3.5° for 16 available discrete phase levels. Note that of the Opto-VLSI processors have a theoretical maximum steering angle of around 6°, however, the maximum steering angle was limited to 3.5° due to the flyback effect in liquid crystal pixel array [13].

We used a tunable light source (Agilent 81689A) followed by a 10 GHz electro optical modulator (JDS Uniphase) which modulates the tunable laser light with an RF signal generated by the network analyser (HP8703A). A 3dB splitter splits the modulated optical signal into two signals: the first is delayed using a fixed fibre length, and the second is fed through a polarization controller and circulator to the micro-delay generator where it is delayed and coupled back into the third port of the circulator, and combined via another 3dB coupler with the first delayed signal. Within the micro-delay generator, the optical beam is collimated at 1 mm diameter by a fibre collimator and arbitrarily delayed by the first Opto-VLSI processor by generating appropriate phase hologram on the Opto-VLSI surface. The beam is then reflected back by the second Opto-VLSI processor along its incident path and the delayed signal is combined with the input non-delayed signal via the second coupler and detected by the photoreceiver of the network analyser. The RF spectrum of the interference between these delayed signals is a notch filter response of centre frequency inversely proportional to the time delay differential between the combined signals, that is $f_c = \frac{c}{nL}$, where n is material refractive index, c is speed of light in vacuum. Therefore, the micro-delay can be calculated by measuring the notch frequency of the RF response measured by the network analyser.

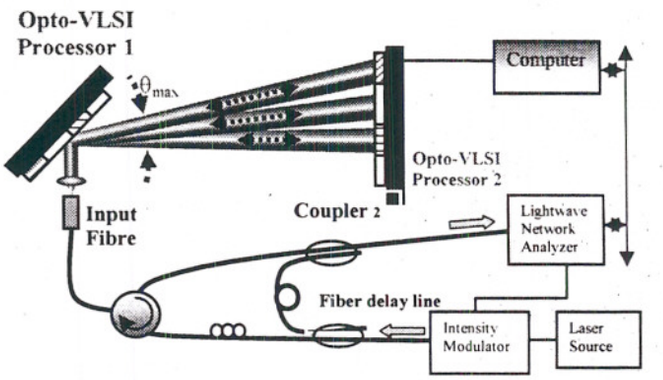

Fig. 3. Experimental setup for micro delay generation.

5. Experimental results

Figure 4 shows the RF responses measured by network analyser (HP8703A) for three different micro-delays corresponding to steering angles θ = 0°, $\theta_{max}/2$ and θ_{max} =3.5°. The measured RF frequencies are: f_1 =2×9.95GHz, f_2 =2×9.82GHz, f_3 =2×9.67GHz, respectively. These correspond to differential path lengths of L_1 =15.075 mm (no steering), L_2 = 15.275 mm (steering angle of $\theta_{max}/2$), and L_3 =15.512 mm (steering angle of θ_{max}), respectively. Therefore, the generated micro-delays are $\Delta L_{12} = L_2 - L_1 = 0.2$ mm, $\Delta L_{13} = L_3 - L_1 = 0.437$ mm.

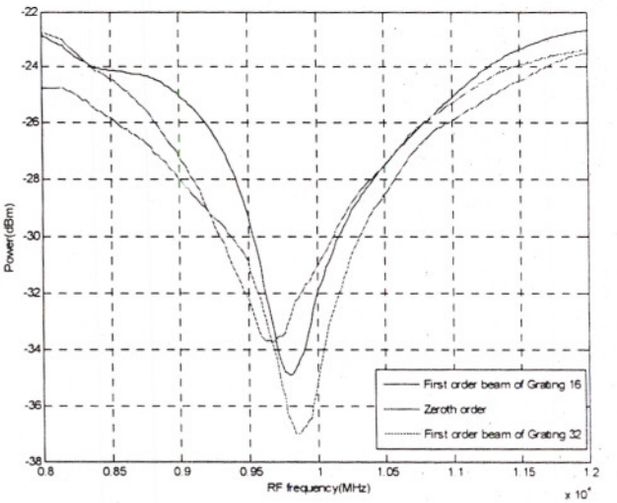

Fig. 4 Measured RF responses for three different microdelays.

In OCT system, a broadband low-coherence light is crucial to obtain high spatial resolution. Figure 5 shows the measured spectral response of the micro-delay generator operating at maximum steering angle. A 3dB bandwidth of 55nm was measured, which is well above the 30 nm bandwidth required for OCT systems. Note that the bandwidth was limited by the round-trip dispersion of the Opto-VLSI processors.

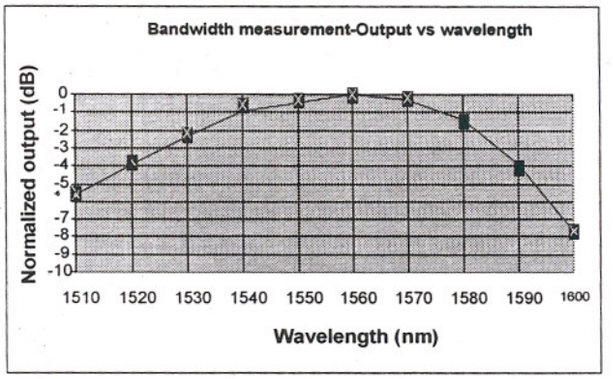

Fig. 5 Spectral response of micro-delay generation

6. Conclusion

A new high resolution motion-free micro-delay generator for Optical Coherence Tomography (OCT) applications has been presented. The generator uses two Opto-VLSI processors to steer optical beams. A theoretical analysis has shown that the design concept has some advantages such as micro depth scanning, high spatial resolution (in micron), broadband spectrum response, flexible scanning depth exchange and multi-depth measurement simultaneously. Proof-of-concept experimental results have demonstrated a maximum delay of 0.5 mm and measured 3dB bandwidth of more than 55 nm.

Acknowledgments

This research was support by the Australian Research Council and The Office of Science and Innovation, Western Australian Government.

References

1. D. Huang, E. A. Swanson, C. P. Lin, J. S. Schuman, W. G.Stinson, W. Chang, M. R. Hee, T. Flotte, K. Gregory, C. A.Puliafito, and J. G. Fujimoto, "Optical coherence tomography," *Science* **254,** 1178–1181 (1991).
2. C. B. Su, "Achieving variation of the optical path length by a few millimeters at millisecond rates for imaging of turbid media and optical interferometry: A new technique," *Opt. Lett.*, vol. 22, pp. 665–667, 1997
3. W. Drexler, U. Morgner, F. X. Ka¨rtner, C. Pitris, S. A. Boppart, X. D. Li, E. P. Ippen, and J. G. Fujimoto, "*In vivo* ultrahighresolution optical coherence tomography," *Opt. Lett.* **24,** 1221– 1223 (1999).
4. A. M. Rollins and J. A. Izatt, "Optimal interferometer designs for optical coherence tomography," *Opt. Lett.* **24,** 1484–1486 (1999)
5. F. Lexer, A. F. Fercher, H. Sattmann, W. Drexler, and S. Molebny, "Dynamic coherent focus for transversal resolution enhancement," *Proc. SPIE*, vol. 3251, pp. 85–90, 1998
6. N. A. Riza, "Scanning heterodyne optical interferometers," *Rev. Sci. Instrum.* **67,** 2466–2476 (1996)
7. N. A. Riza, "Acousto-optically switched optical delay lines," *Opt. Commun.* **145,** 15–20 _1998_.
8. N. A. Riza and Z. Yaqoob, "Submicrosecond speed optical coherence tomography system design and analysis by use ofacousto-optics".*Applied Optics* Vol.42 3018-3027 (2003)
9. E. N. Leith, C. Chen, H. Chen, Y. Chen, D. Dilworth, J. Lopez, J. Rudd, P.C. Sun, J. Valdmanis, and G. Vossler, "Imaging through scattering media with holography," *J. Opt. Soc. Amer. A*, vol. 9, pp. 1148–1153, 1992.
10. A. Kn¨uttel, J. M. Schmitt, and J. R. Knutson, "Low-coherence reflectometry for stationary lateral and depth profiling with acousto-optic deflectors and a CCD camera," *Opt. Lett.*, vol. 19, pp. 302–304, 1994.
11. Rong Zheng, Zhenglin Wang, Kamal E. Alameh, and William A. Crossland. "An Opto-VLSI Reconfigurable Broad-Band Optical Splitter". *IEEE Photonics Tech. Lett., vol.* 17, P339, 2005
12. H. Dammann, "Spectral characteristics of stepped-phase gratings", *Optik*, Vol. 53, pp 409-417, 1979
13. M.Bouvier,T.Scharf, "Analysis of nematic-liquid-crystal binary gratings with high spatial frequency", *Opt.Eng*.39(8), pp.2129-2137, 2000.